



HAL
open science

Modelling temporal variation of parameters used in two photosynthesis models: influence of fruit load and girdling on leaf photosynthesis in fruit-bearing branches of apple

Magalie Poirier-Pocovi, Jérémy Lothier, Gerhard G. Buck-Sorlin

► To cite this version:

Magalie Poirier-Pocovi, Jérémy Lothier, Gerhard G. Buck-Sorlin. Modelling temporal variation of parameters used in two photosynthesis models: influence of fruit load and girdling on leaf photosynthesis in fruit-bearing branches of apple. *Annals of Botany*, 2018, 21 (5), pp.821-832. 10.1093/aob/mcx139 . hal-01904786

HAL Id: hal-01904786

<https://hal.science/hal-01904786>

Submitted on 4 Sep 2019

HAL is a multi-disciplinary open access archive for the deposit and dissemination of scientific research documents, whether they are published or not. The documents may come from teaching and research institutions in France or abroad, or from public or private research centers.

L'archive ouverte pluridisciplinaire **HAL**, est destinée au dépôt et à la diffusion de documents scientifiques de niveau recherche, publiés ou non, émanant des établissements d'enseignement et de recherche français ou étrangers, des laboratoires publics ou privés.

Copyright

PART OF A SPECIAL ISSUE ON FUNCTIONAL–STRUCTURAL PLANT GROWTH MODELLING
**Modelling temporal variation of parameters used in two photosynthesis models:
influence of fruit load and girdling on leaf photosynthesis in fruit-bearing
branches of apple**

Magalie Poirier-Pocovi*, Jérémy Lothier and Gerhard Buck-Sorlin

IRHS, INRA, AGROCAMPUS-OUEST, Université d'Angers, SFR 4207 QUASAV, 42 rue Georges Morel, F-49071 Beaucozéd
cedex, France

*For correspondence. E-mail: magalie.poirier@laposte.net

Received: 13 March 2017 Returned for revision: 23 August 2017 Editorial decision: 20 September 2017 Accepted: 2 November 2017
Published electronically 4 January 2018

- **Background and Aims** Several studies have found seasonal and temporal variability in leaf photosynthesis parameters in different crops. This variability depends upon the environment, the developmental stage of the plant and the presence or absence of sinks. Girdling involves the removal of the bark and phloem down to the youngest xylem all around the stem and prevents export of photoassimilates out of the stem. The load of developing fruits has often been reported to influence the individual net leaf photosynthesis rate (P_n) in tree crops. In this study, we chose (1) to model the key parameters of photosynthesis models of leaves ($P_{g_{max}}$, R_d , α and θ) as a function of time and using these two means (girdling and low fruit load) to alter the source–sink balance and (2) to compare three models: the rectangular and non-rectangular hyperbola model by Thornley, as well as the non-rectangular hyperbola model by Marshall and Biscoe.
- **Methods** Six-year-old fruit-bearing branches of 10-year-old apple trees were used to study and model the seasonal variation of photosynthetic parameters in leaves of vegetative shoots, as a function of global fruit load (at the branch level), with or without girdling, during the growing season of 2015. Three treatments were applied: control, low load (LL) or low load + girdling (LLG). For each fruit-bearing branch, light–response curves of P_n for two leaves of vegetative shoots were measured at two different positions, proximal and distal.
- **Key Results** The model of Marshall and Biscoe was the most accurate for the simulation of P_n in fruit-bearing branches of apple trees with time (season) and the three treatments applied.
- **Conclusion** The present study proposed a way to model the photosynthesis rate by temporal and environmental variables only. A proper validation of this model will be necessary to extend its utilization and appreciate its predictive capacity fully.

Key words: Net photosynthesis rate, modelling, shoot leaf, photosynthetic parameter, fruit load, dark respiration, gross photosynthesis rate, Thornley's model, Marshall and Biscoe's model, *Malus domestica*

INTRODUCTION

Photosynthesis is the process whereby green plants utilize a portion of the photon energy from the sun to drive endergonic reactions that store chemical energy. Over the last 50 years, knowledge and understanding of the metabolism of carbon, as well as its apparent complexity, have increased considerably. Besides carbon reduction, chemical energy produced by photosynthesis is used for all processes in the plant cell, primary and secondary metabolism. Photosynthesis, like all complex metabolic processes, is subject to metabolic regulations, with the main activator being visible light [photosynthetically active radiation (PAR)] (Hopkins, 2003). Generally, the photosynthesis rate increases in spring. The maximum value is reached after completion of leaf expansion. It is relatively constant during the summer period and finally declines in autumn during leaf senescence (Wang *et al.*, 2008; Dillen *et al.*, 2012; Sun *et al.*, 2015).

In this study, girdling and fruit load are only used as means to alter the source–sink balance. Girdling treatment involves the removal of the bark and phloem down to the youngest xylem

all around the stem to prevent the export of photoassimilates from the stem (Poirier, 2008; Fan *et al.*, 2010), while still permitting water transport in the reverse direction through the xylem for an extended period, up to several months (Högberg *et al.*, 2001; Binkley *et al.*, 2006). This technique is often used to study carbon relationships and to alter source–sink relationships. Girdling has been shown to decrease the photosynthesis rate in several tree species (Iglesias *et al.*, 2002; Zhou and Quebedeaux, 2003; Urban *et al.*, 2004; Nebauer *et al.*, 2011). This reduction may be due to a feedback inhibition of photosynthesis when girdling-induced accumulation of photoassimilates exceeds demand (Iglesias *et al.*, 2002; Mialet-Serra *et al.*, 2008; Franck and Vaast, 2009; Asao and Ryan, 2015). Furthermore, girdling affects photosynthesis permanently by decreasing the leaf nitrogen concentration (Urban *et al.*, 2004).

The load of developing fruits on a branch has often been reported to have an influence on individual leaf photosynthesis rate in tree crops (Palmer, 1992; Palmer *et al.*, 1997; Wünsche *et al.*, 2005). The primary effect of fruit on CO₂ assimilation

in *Prunus persica* is through effects on stomatal regulation of CO₂ and H₂O exchange (DeJong, 1986). Low fruit load exerts a negative effect on the photosynthesis rate by decreasing the amount of nitrogen per unit leaf area and leaf nitrogen concentration, and by affecting the relationship between the maximal rate of carboxylation and the light-saturated rate of photosynthetic electron transport, and the amount of nitrogen per unit leaf area (Urban *et al.*, 2004). In *Olea europaea* L., net photosynthesis may remain high when sink activity (i.e. growing fruits) is strong (Proietti and Tombesi, 1990; Proietti, 2000). However, Urban *et al.* (2004) point out that a high fruit load in *Mangifera indica* L. does not totally counterbalance the negative effect of girdling on photosynthesis.

Models of photosynthesis play a major role in defining the path towards understanding of photosynthetic carbon uptake. Several studies describe the light (PAR) response curve of the leaf net photosynthesis rate (P_n) [$P_n = f(\text{PAR})$]. The most common functions for $f(\text{PAR})$ are the rectangular hyperbola (RH; Thornley, 1998) and non-rectangular hyperbola (NRH; Thornley, 1998; Marshall and Biscoe, 1980) models. These models have few parameters, which can be defined easily. The NRH gives an excellent phenomenological description of leaf photosynthesis, whereas the RH has been shown to be a rather poor description of the response of photosynthesis to irradiance for leaves of a winter wheat crop (Marshall and Biscoe, 1980).

A large number of studies have found seasonal variability in leaf photosynthesis parameters (maximum carboxylation rate, dark respiration, maximum electron transport capacity and light-saturated photosynthesis) in different crops (Wilson *et al.*, 2001; Xu and Baldocchi, 2003; Grassi *et al.*, 2005; Feng *et al.*, 2011; Dillen *et al.*, 2012; Yang *et al.*, 2013). Few modelling studies on woody plants take into account (1) seasonal and temporal variation of photosynthetic parameters (Auzmendi, 2013 on *Malus domestica* Borkh. and *Pyrus communis* L.), in particular the model parameters α and θ , and (2) none of them proposes to simulate the effects of fruit load (sinks), coupled or not with girdling, on the photosynthesis rate of the leaf (sources) over time. In this study, we focus on the seasonal variation in the photosynthetic parameters [maximum gross photosynthesis rate ($P_{g_{\max}}$), dark respiration (R_d), α and θ] in vegetative shoot leaves of the apple tree cultivar ‘Elstar’ under production conditions in the orchard.

The aims of this study were thus (1) to model the key parameters of photosynthesis models of leaves ($P_{g_{\max}}$, R_d , α and θ) as a function of time; (2) to compare three photosynthesis models [Thornley’s RH model (Thornley, 1998), Thornley’s NRH model (Thornley, 1998) and Marshall and Biscoe’s model (Marshall and Biscoe, 1980)] to determine which model best described the variation of photosynthesis parameters over the vegetative season in apple trees subject to certain treatments (low fruit load and girdling); and (3) to establish some additional information on the effect of these treatments on the sink–source relationship.

MATERIALS AND METHODS

Plant material

This study was performed in 2015 on four 10-year-old apple trees (*Malus domestica* ‘Elstar’) trained under production conditions based on sufficient water and nitrogen supply (culture conditions

used by the orchardists in the Pays de la Loire region, sustainable cultural practice) in an experimental orchard at the INRA site of Beaucouzé, North West of France (altitude: 47 m, on average; 47°29’N, 0°36’W). In the experimental plot, full bloom occurred during week 16 (18 April 2015). In order to avoid additional stress during the treatments, all preparatory measures were conducted on the experimental trees well before the start of the treatments (control, low load and low load + girdling) and fruits were just thinned naturally. Three 6-year-old fruit-bearing branches were selected on each tree, with different insertion orientations on the trunk. During summer 2015, each one of the selected fruit-bearing branches was treated independently. On one branch, fruit load was reduced by reducing the total number of fruits to one-third (100 % leaves with 33 % fruits); all fruits were concentrated in the basal third of the branch (Z1), near the trunk [low load, LL, 0.9 ± 0.3 fruits mm⁻¹ (branch diameter at its base), Fig. 1A, C], and the upper two-thirds of the branch (Z2, apical part of the branch) bore no fruit. A second branch was reduced in its fruit load (as before, the same zones were defined) and girdled near the trunk, i.e. the bark, including phloem, was removed all around the branch [low load + girdling (G), LLG, 0.6 ± 0.2 fruits mm⁻¹, Fig. 1A]. The last fruit-bearing branch of the tree was left untreated as control (control, 100 % leaves with 100 % fruits, 3.1 ± 1.3 fruits mm⁻¹, Fig. 1A, B) and the same two zones were defined (Z1 and Z2). Treatments were applied on branches randomly, from 10 weeks after full bloom (WAFB) to 24 WAFB. The growing season was divided into four dates/periods: WAFB 10 [marking the end of primary shoot (extension) growth and the period before the application of treatments]; WAFB 11–20 (from the end of active shoot growth to fruit harvest, thus after the application of treatments and before fruit harvest); WAFB 21–22 (immediately after fruit harvest); and WAFB 23–24 (until the beginning of leaf shedding). Fruit harvest of treated branches was done in WAFB 21 (8 September 2015).

Photosynthetic capacity

Gas exchange measurements were carried out using a LI-6400XT portable photosynthesis system (LiCor, Inc., Lincoln, NE, USA). For each fruit-bearing branch, we measured light–response curves of P_n [$P_n = f(\text{PAR})$] for two marked leaves of a vegetative shoot (Fig. 1D): one marked leaf was located in the middle of Z1 and another marked leaf was situated in the middle of Z2. Twenty-four leaves were selected following several criteria: fully expanded, on the vegetative shoot (Fig. 1D), positioned in full sun, the same angle position and the same size. A part of each leaf was placed across a 2 × 3 cm cuvette that was equipped with an LED light source (6400-02B, LiCor, Inc.). Leaf incident PAR values were set to the following values ($\mu\text{mol photons m}^{-2} \text{ s}^{-1}$): 2000, 1500, 1000, 500, 250, 100, 50, 25 and 0. The light–response curves of P_n were measured at a CO₂ concentration of 400 $\mu\text{mol CO}_2 \text{ mol}^{-1}$. The value of P_n was recorded once we had obtained the stabilization of the value (plateau). Inside the cuvette, leaf temperature was maintained at 20 °C and relative humidity at about 60 %. Dark respiration (R_d) was taken as P_n when PAR was zero. Because of the large number of data points, the measurements were done on several days during the week. Measurements carried out on the same tree were also measured on the same day. All measurements were realized in the morning from 8.00 h to 11.00 h and were repeated on the

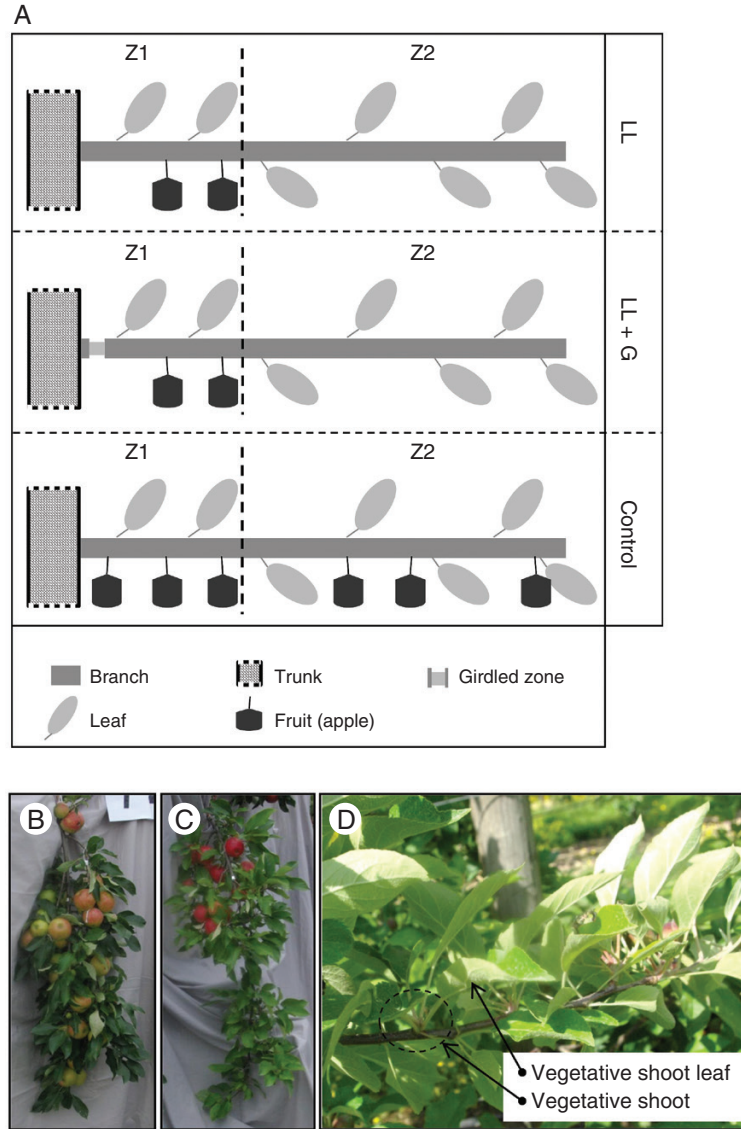


FIG. 1. (A) Schematic representation of the three treatments: control, low load (LL) and low load + girdling (LLG) (Z1, zone 1; Z2, zone 2). Photographs of fruit-bearing branches with ‘control’ treatment (B), with ‘low load (LL)’ treatment (C) and of the type of leaf named ‘vegetative shoot leaf’ in our study (D) (i.e. this structure does not bear fruit).

same marked leaves during the experimental period. The weeks of measurement were WAFB 10, 12, 15, 18, 21 and 24 (Fig. 2). For LLG, the measurements started at WAFB 15.

Description of models

Rectangular hyperbola and non-rectangular hyperbola (Thornley). Leaf gross photosynthetic rate, P_g ($\mu\text{mol CO}_2 \text{ m}^{-2} \text{ s}^{-1}$), depends upon the light incident on the upper leaf surface, PAR ($\mu\text{mol photons m}^{-2} \text{ s}^{-1}$), according to an NRH:

$$\theta P_g^2 - (\alpha \text{PAR} + P_{g_{\max}}) P_g + \alpha \text{PAR} P_{g_{\max}} = 0 \quad (1)$$

where θ (dimensionless) determines the sharpness of the knee of the curve; α is the initial slope of the light–response curve;

$P_{g_{\max}}$ is the instantaneous high-light asymptote of Eqn (1): $\text{PAR} \rightarrow \infty, P_g \rightarrow P_{g_{\max}}$. $P_{g_{\max}}$ is defined as follows:

$$P_{g_{\max}} = P_{n_{\max}} + R_d \quad (2)$$

R_d ($\mu\text{mol CO}_2 \text{ m}^{-2} \text{ s}^{-1}$) is the dark respiration at $\text{PAR} = 0 \mu\text{mol photons m}^{-2} \text{ s}^{-1}$. $P_{n_{\max}}$ ($\mu\text{mol CO}_2 \text{ m}^{-2} \text{ s}^{-1}$) is the leaf net photosynthetic rate at $\text{PAR} = 2000 \mu\text{mol photons m}^{-2} \text{ s}^{-1}$. These two values were measured *in vivo* in the field with the LI-6400XT portable photosynthesis system. The model, as it appears in Eqn (1), is in quadratic form and can be rewritten:

$$a P_g^2 + b P_g + c = 0 \quad (3)$$

where $a = \theta$, $b = -(\alpha \text{PAR} + P_{g_{\max}})$ and $c = \alpha \text{PAR} P_{g_{\max}}$.

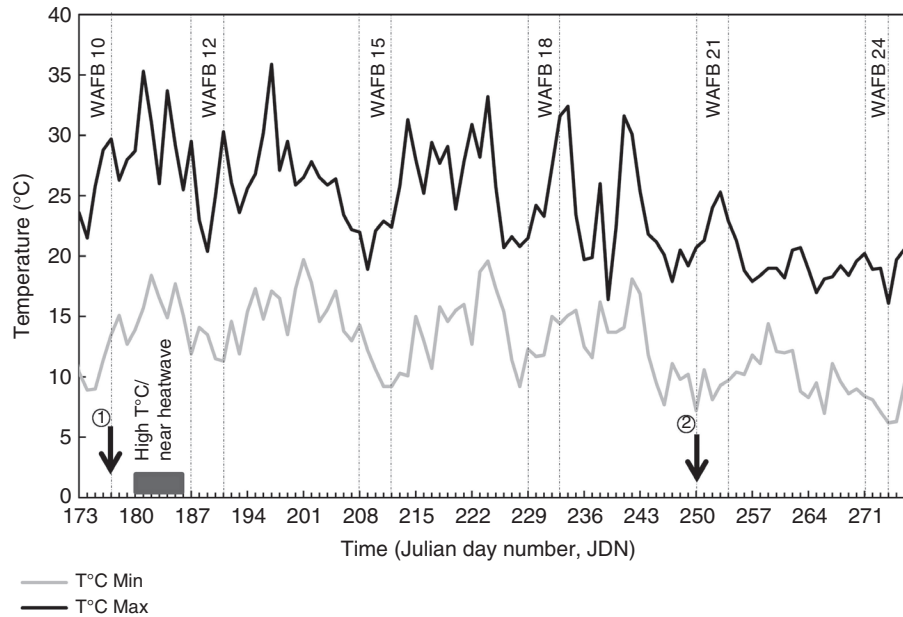


FIG. 2. Time courses of daily minimum and maximum air temperatures at the INRA site of Beaucouzé. The dotted line indicates the measurement periods of P_n . WAFB is the number of weeks after full bloom. The black box shows a period with high temperatures (almost a heatwave). The arrow marked 1 indicates application of treatments and that marked 2 indicates fruit harvest.

The NHR of Eqn (1) is quadratic in P_g , with the solution:

$$P_g = \frac{\alpha PAR + P_{g_{\max}} - \sqrt{-(\alpha PAR + P_{g_{\max}})^2}}{-4\theta \alpha PAR P_{g_{\max}}} \quad (4)$$

Thornley's RH model (Thornley, 1998) is a special case of Thornley's NRH model. It can be obtained from the NRH model by setting $\theta = 0$ in Eqn (4); this involves taking the limit as $\theta \rightarrow 0$ and is rather tedious. It is easier to put $\theta = 0$ in Eqn (1) which immediately gives the RH model:

$$P_g = \frac{\alpha PAR P_{g_{\max}}}{\alpha PAR + P_{g_{\max}}} \quad (5)$$

Marshall and Biscoe's model. Marshall and Biscoe's model (Marshall and Biscoe, 1980) describes the dependence of P_n on irradiance (PAR), according to an NRH:

$$aP_n^2 + bP_n + c = 0 \quad (6)$$

The model as it appears in Eqn (6) is in quadratic form and can be rewritten:

where $a = \theta$, $b = -(\alpha PAR + P_{g_{\max}} - \theta Rd)$ and $c = \alpha PAR [P_{g_{\max}} - (1 - \theta)Rd] - Rd P_{g_{\max}}$.

The NRH of Eqn (6) is quadratic in P_n , with the solution

$$P_n = \frac{\alpha PAR + P_{g_{\max}} - \theta Rd - \sqrt{-(\alpha PAR + P_{g_{\max}} - \theta Rd)^2 - 4\theta(\alpha PAR (P_{g_{\max}} - (1 - \theta)Rd) - Rd P_{g_{\max}})}}{2\theta} \quad (7)$$

$P_{g_{\max}}$, Rd , α and θ have the same meaning as in Thornley's NRH model.

These models were chosen as they are simple (few parameters that are easy to measure: $P_{g_{\max}}$, Rd , α and θ). The non-linear solver routine in Microsoft Excel 2010 (Microsoft Office Professional Plus 2010) was used to model the light-response curves and calculate the values of α and θ from the measured light-response curves.

Meteorological data

Daily minimum and maximum air temperatures for the period from 22 June 2015 [Julian day number (JDN) 173] to 4 October 2015 (JDN 277) were obtained from the weather station Beaucouzé (Météo France), which is situated near the experimental site at Beaucouzé (47°29'N, -0°35'E) (https://intranet.inra.fr/climatik_v2).

Statistical analysis

Averages were calculated from the individual values. Results were expressed as average \pm s.d. (Weissgerber et al., 2015). As the sample size was small ($n = 4$), the significance of differences between averages was evaluated by the non-parametric tests: Mann-Whitney test (comparison of two independent groups, i.e. the difference between zones), Kruskal-Wallis test (comparison of more than two independent groups, i.e. the difference between treatments for a given date) and Friedman's test (repeated measures, i.e. the difference between dates for a given treatment).

The goodness-of-fit of models was evaluated using three statistics.

- (1) The coefficient of determination, adjusted for estimated parameters (Hill and Lewicki, 2007; Dincer and Topuz, 2015) to yield an unbiased value, R^2_{adj} .
- (2) The index of agreement d is a standardized measure of the degree of model prediction error and varies between 0 and 1. A value of 1 indicates a perfect match, while 0 indicates no agreement at all. It is defined in Willmott (1982) as:

$$d = 1 - \frac{\sum_{i=1}^n (P_i - O_i)^2}{\sum_{i=1}^n (|P_i| + |O_i|)^2}, 0 \leq d \leq 1 \quad (8)$$

where $P_i' = P_i - \bar{O}$, $O_i' = O_i - \bar{O}$, \bar{O} is the mean of observed values and O_i and P_i are the i th observed and i th corresponding model-predicted variables, respectively.

- (3) The quadratic mean deviation estimated from measured values, or root mean squared error, RMSE (Janssen and Heuberger, 1995).

For parameterization, we used three-quarters of the presented data (three trees were chosen at random). The rest of the data (the remaining tree) and other measurements of P_n on cultivar 'Elstar' carried out at the same time were used for a preliminary model validation (because of the limited validation power of our model parameters). The predictive capacity was evaluated by validation on data sets that were not used to parameterize the model (see above), using the same three indices: R^2_{adj} , d and RMSE, here referred to as the RMSE of prediction (RMSEP).

RESULTS

Thermal conditions during experimentation time

The experimental site is characterized by a climate intermediate between oceanic and continental. Variations of daily minimum and maximum air temperatures between 30 June 2015 and 4 October 2015 are shown in Fig. 2. Before harvest, the average daily minimum and maximum air temperatures during the experimental period were 13.7 ± 0.3 °C ($n = 78$) and 25.7 ± 0.5 °C ($n = 78$), respectively. After harvest, they were 9.6 ± 0.4 °C ($n = 27$) and 19.5 ± 0.4 °C ($n = 27$), respectively. Punctually, the daily maximum air temperature was >32 °C (JDN 181, 184, 197, 224 and 234). During WAFB 11, the daily air temperature was close to heatwave conditions. Twice in the same week (JDN 181 and 184), the daily maximum air temperature was >35 °C and the daily minimum air temperature was >17 °C. After JDN 242, the daily maximum air temperature decreased and rarely reached 25 °C.

Leaf development

On 7 October 2015 (WAFB 25), the leaves on girdled fruit-bearing branches were brownish yellow, while the leaves in ungirdled fruit-bearing branches were still green.

Effect of treatments on light–response curves of net photosynthesis over time

Before treatments (WAFB 10, Fig. 3A), the $P_{n_{\text{max}}}$ of the leaves in Z2 was significantly higher than the $P_{n_{\text{max}}}$ of the leaves in Z1 (17.8 ± 0.7 and 15.8 ± 0.4 $\mu\text{mol CO}_2 \text{ m}^{-2} \text{ s}^{-1}$, respectively; $P = 0.016$). After treatments and before harvest (Fig. 3B–D), there was no significant difference between these two zones ($P > 0.05$). 'LL' treatment had no significant effect on the shape of the light–response curve of P_n ($P > 0.05$). $P_{n_{\text{max}}}$ reached about $17 \mu\text{mol CO}_2 \text{ m}^{-2} \text{ s}^{-1}$. However, 'LLG' treatment induced a significant decrease of P_n above a PAR of $500 \mu\text{mol photons m}^{-2} \text{ s}^{-1}$ ($P < 0.05$; Fig. 3C, D) and was maintained above $13.5 \mu\text{mol CO}_2 \text{ m}^{-2} \text{ s}^{-1}$. For a PAR of $2000 \mu\text{mol photons m}^{-2} \text{ s}^{-1}$, this treatment caused a reduction of about 26–32 % of $P_{n_{\text{max}}}$ at WAFB 15–18, respectively. After harvest (WAFB 21, Fig. 3E), P_n decreased. For the leaves in Z2, there was no significant difference between the P_n of the 'control' treatment and the P_n of the 'LL' treatment. $P_{n_{\text{max}}}$ decreased by 13.5 %, on average, between WAFB 18 and WAFB 21 for these two treatments. For the leaves in Z1 (i.e. where the fruits were located), $P_{n_{\text{max}}}$ decreased more rapidly (30 % for 'control Z1' and 41 % for 'LL Z1'). $P_{n_{\text{max}}}$ in 'LL Z1' was significantly less than in 'control Z2' and 'LL Z2'. For the 'LLG' treatment, from a PAR of $100 \mu\text{mol photons m}^{-2} \text{ s}^{-1}$, P_n declined drastically and significantly ($P_n < 2.6 \mu\text{mol CO}_2 \text{ m}^{-2} \text{ s}^{-1}$, $P < 0.003$). Three weeks after harvest (WAFB 24, Fig. 3F), P_n values continued to decrease and became less than about $9.9 \mu\text{mol CO}_2 \text{ m}^{-2} \text{ s}^{-1}$. The 'LL Z1' treatment exhibited a slightly (but significantly: $P < 0.05$) lower $P_{n_{\text{max}}}$ than 'LL Z2' treatment. This difference was not significant between 'control Z1' and 'control Z2'. P_n values of the girdled treatment became $<1.3 \mu\text{mol CO}_2 \text{ m}^{-2} \text{ s}^{-1}$. This treatment is significantly lower than other treatments. We also observed that the decrease in $P_{n_{\text{max}}}$ in autumn coincided with the decrease of daily minimum and maximum air temperatures (Figs 2 and 3).

Modelling the time course of $P_{g_{\text{max}}}$, R_d , α and θ for different treatments

The course of $P_{g_{\text{max}}}$ between WAFB 10 and WAFB 24 for three treatments and two zones on the fruit-bearing branches is shown in Fig. 4. Before treatment (WAFB 10), $P_{g_{\text{max}}}$ of leaves in Z2 was significantly higher than $P_{g_{\text{max}}}$ of leaves in Z1 ($P = 0.015$). Therefore, for WAFB 10, one average was calculated for each zone (Table 1). After treatments, the course of $P_{g_{\text{max}}}$ exhibited various patterns for treatments and zones. In the control, no zone effect was detected throughout the experiment ($P > 0.11$). Thus, one non-linear curve (sigmoid curve) represented the course of $P_{g_{\text{max}}}$ in the control (Table 1). For 'LL', a significant effect of zone was detected throughout the experiment (WAFB 15, $P = 0.001$; WAFB 21 and WAFB 24, $P = 0.038$). Accordingly, two non-linear (sigmoid) curves were used to represent the course of $P_{g_{\text{max}}}$ for 'LL' (Table 1) and both zones. For 'LLG', no effect of zone was detected throughout the experiment ($P > 0.31$). Therefore, only a single non-linear (sigmoid) curve was used for the representation of the course of $P_{g_{\text{max}}}$ for 'LLG' (Table 1). All proposed models used to simulate $P_{g_{\text{max}}}$ in the different treatments and zones explained a satisfactory percentage of the variance

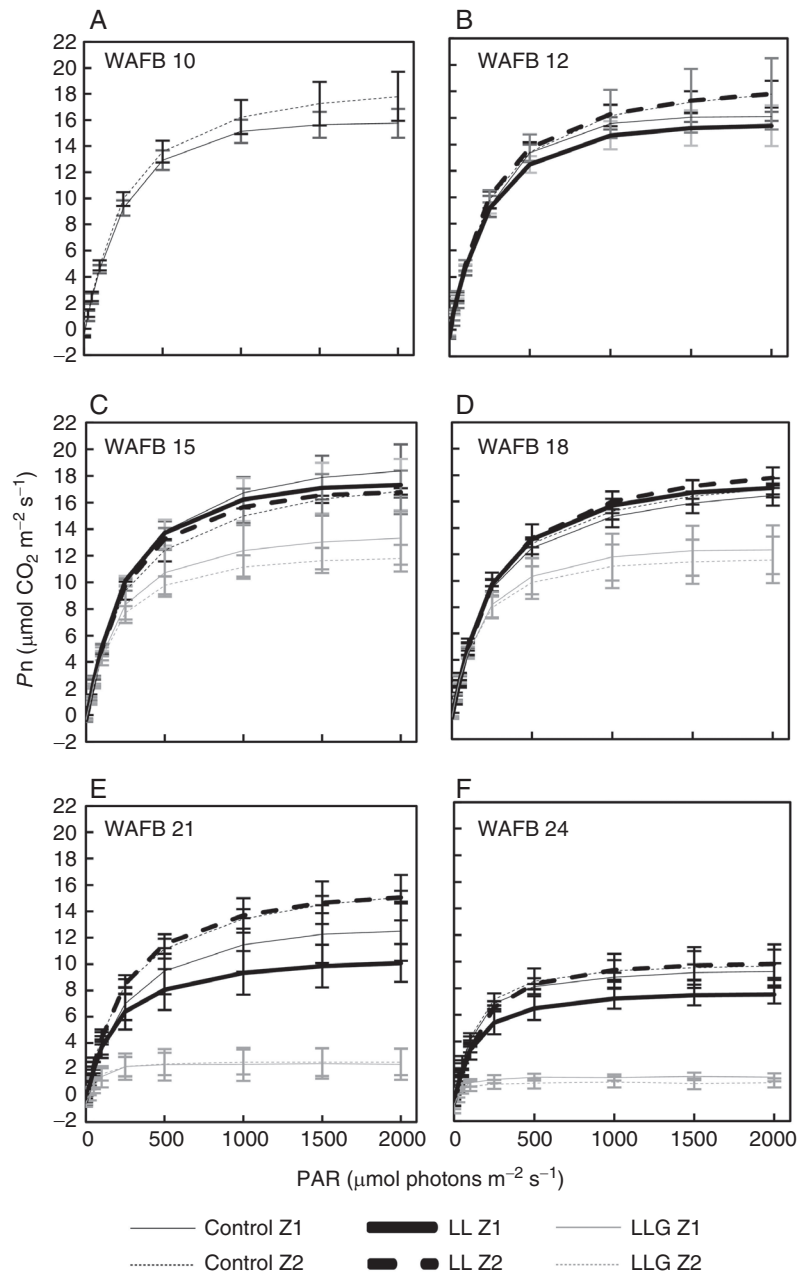


FIG. 3. Time course of light response curve of P_n [$P_n = f(\text{PAR})$] of vegetative shoot leaves (Fig. 1D) (average \pm s.d., $n = 4$, 10 weeks after full bloom = WAFB 10; $n = 8$) for different fruit load and girdling treatments. (A) Before treatments (WAFB 10), (B–D) after treatments and before fruit harvest (WAFB 12, WAFB 15 and WAFB 18), (E) after fruit harvest (WAFB 21) and (F) 3 weeks after harvest (WAFB 24). Fruit harvest was carried out in WAFB 21 (8 September 2015).

($R^2_{\text{adj}} = 0.87$, $P < 0.001$). Overall, the mean residual error of fitting (RMSE) was $\pm 1.90 \mu\text{mol CO}_2 \text{ m}^{-2} \text{ s}^{-1}$. The mean prediction error (RMSEP) was $\pm 1.97 \mu\text{mol CO}_2 \text{ m}^{-2} \text{ s}^{-1}$ ($n = 32$), showing its applicability to data independent of those which had been used to build it (Table 2).

Variation of R_d between WAFB 10 and WAFB 24 for three treatments and two zones on fruit-bearing branches is shown in Fig. 5. Over the course of time and for each defined date (significant difference between the dates, $P < 0.02$), there were no significant differences between Z1 and Z2 or between the treatments ($P > 0.05$) (Fig. 5). R_d attained $0.574 \pm 0.048 \mu\text{mol CO}_2$

$\text{m}^{-2} \text{ s}^{-1}$ ($n = 4$), on average, before treatment (WAFB 10), then decreased quickly and stabilized at $0.343 \pm 0.017 \mu\text{mol CO}_2 \text{ m}^{-2} \text{ s}^{-1}$ ($n = 4$) from WAFB 12 to 18. After harvest, R_d increased slightly, to $0.452 \pm 0.057 \mu\text{mol CO}_2 \text{ m}^{-2} \text{ s}^{-1}$ ($n = 4$). This increase allowed R_d to reach, 3 weeks after harvest, a value of $0.607 \pm 0.090 \mu\text{mol CO}_2 \text{ m}^{-2} \text{ s}^{-1}$ ($n = 4$). For WAFB 24, ‘LLG’ treatment might suggest an increasing trend of R_d faster than other treatments (no significant increase). Thus, for each date (WAFB 10, WAFB 11–20, WAFB 21–22 and WAFB 23–24) a single value (an average) was calculated for model calibration (Table 1). The RMSE was $\pm 0.12 \mu\text{mol CO}_2 \text{ m}^{-2} \text{ s}^{-1}$. RMSEP was

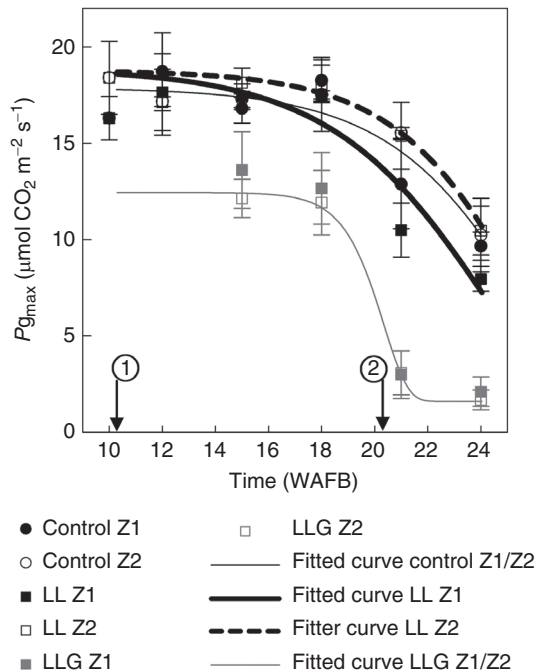


FIG. 4. Time course of $P_{g_{max}}$ of vegetative shoot leaves (Fig. 1D) (average \pm s.d., $n = 4$, WAFB 10: $n = 8$) for different fruit load and girdling treatments. The arrow marked 1 indicates application of treatments and that marked 2 indicates fruit harvest. Fruit harvest was carried out in WAFB 21 (8 September 2015).

still quite acceptable: $\pm 0.25 \mu\text{mol CO}_2 \text{ m}^{-2} \text{ s}^{-1}$ on values ranging from 0.2 to $1.7 \mu\text{mol CO}_2 \text{ m}^{-2} \text{ s}^{-1}$ (Table 2). Moreover, a higher variability of R_d values was observed after harvest (Fig. 5).

The course of α of Thornley's NRH model between WAFB 10 and WAFB 24 for three treatments and two zones on fruit-bearing branches is shown in Fig. 6A. No effect of zone was detected throughout the experiment and for all treatments ($P > 0.06$), except for 'LLG' at WAFB 24. The same model was used to explain the temporal variation of α for both zones, except for 'LLG'. In the control, no significant effect ($P > 0.07$) of time was found, and there was no discernible seasonal pattern. Therefore, the mean (0.0568 ± 0.0055) was used to simulate this parameter. For 'LL', a significant effect ($P < 0.03$) of time was detected. Thus, one linear curve represented the course of this α (Table 1). Finally, a significant effect ($P < 0.001$) of time was also identified for 'LLG'. This led us to use two non-linear (sigmoid) curves to represent the course of α for 'LLG' in Z1 and Z2 (Table 1). Overall, for the simulation of temporal variation of this α for three treatments and two zones, RMSE and RMSEP were ± 0.006 and $\pm 0.007 \mu\text{mol CO}_2 \mu\text{mol photons}^{-1}$, respectively (Table 2).

The course of α of Marshall and Biscoe's NRH model between WAFB 10 and WAFB 24 for three treatments and two zones on fruit-bearing branches is shown in Fig. 6B. No effect of treatments was detected throughout the experiment ($P < 0.08$), though a wide variation was apparent among the individual values on WAFB 21 and WAFB 24. There was no discernible seasonal pattern. Thus, α was defined by the average of all values and fixed at $0.056 \pm 0.011 \mu\text{mol CO}_2 \mu\text{mol photons}^{-1}$. The RMSE and RMSEP were ± 0.011 and $\pm 0.009 \mu\text{mol CO}_2 \mu\text{mol photons}^{-1}$, respectively (Table 2).

The course of α of Thornley's RH model between WAFB 10 and WAFB 24 for three treatments and two zones on fruit-bearing branches is shown in Fig. 6C. During the experimental period, α ranged from 0.111 to $0.06 \mu\text{mol CO}_2 \mu\text{mol photons}^{-1}$ (on average). No zone effect was detected throughout the experiment and for all treatments ($P > 0.14$). Therefore, the same model was used to explain the temporal variation of this α for both zones. No discernible seasonal pattern was detected, either for treatment or for a particular period (Fig. 6C). Four periods were defined: WAFB10, WAFB 11–20, WAFB 21–22 and WAFB 23–24 and the means were used to simulate this parameter within each period (Table 1 for values). The RMSE and RMSEP were ± 0.011 and $\pm 0.014 \mu\text{mol CO}_2 \mu\text{mol photons}^{-1}$, respectively (Table 2).

The course of θ of Thornley's NRH model between WAFB 10 and WAFB 24 for three treatments and two zones on fruit-bearing branches is shown in Fig. 6D. Before treatments (WAFB 10), there was a statistically significant difference ($P = 0.038$) between both zones. Accordingly, two averages were used to simulate θ (Table 1). After treatments, no treatment effect was detected throughout the experiment ($P > 0.06$). There was no discernible seasonal pattern. Therefore, θ of Thornley's NRH model was defined by the average of all values (0.721 ± 0.092). Overall, RMSE and RMSEP were ± 0.089 and ± 0.09 , respectively (Table 2).

Variation of θ of Marshall and Biscoe's NRH model between WAFB 10 and WAFB 24 for three treatments and two zones on fruit-bearing branches is shown in Fig. 6E. For 'LLG', no significant effect ($P > 0.31$) of zone yet a significant effect ($P < 0.012$) of time were detected. This led us to use a non-linear (sigmoid) curve to represent the course of θ for this treatment and both zones (Table 1). In the control, a significant effect ($P < 0.03$) of zone was detected in WAFB 21 and, for Z1, there was a significant effect of time ($P = 0.051$). Therefore, two linear curves were used to simulate the seasonal variation of this parameter (Table 1). Finally, for 'LL', a significant effect ($P < 0.006$) of time in Z1 was detected, thus a linear curve represented the course of θ for this treatment. In Z2, a mean was used ($\theta = 0.711 \pm 0.062$). Overall, for the simulation of this θ in these three treatments and two zones, RMSE and RMSEP were ± 0.095 for both (Table 2).

Comparison between the models of Marshall/Biscoe and Thornley

Table 3 summarizes the statistical evaluation and the comparison of three models used with our parameter set. The best model yielding the P_n of leaves on the fruit-bearing branches with time and three treatments applied is the model of Marshall and Biscoe. This model and our parameter set explained a very good percentage of variance ($R^2_{adj} = 0.963$). The RMSE was $\pm 1.182 \mu\text{mol CO}_2 \text{ m}^{-2} \text{ s}^{-1}$. The RMSEP was $\pm 1.575 \mu\text{mol CO}_2 \text{ m}^{-2} \text{ s}^{-1}$ on values ranging from -1.1 to 20.3.

DISCUSSION

Seasonal variation of P_n , $P_{g_{max}}$ and R_d

During the course of our experiment, P_n and $P_{g_{max}}$ showed clear seasonal dynamics. These dynamics are typical seasonal patterns, with increasing rates in the early season until developing

TABLE 1. Values of parameters used in the models of Pg_{\max} , Rd , α and θ for three treatments [control, low load (LL) and low load + girdling (LLG)] and two zones [zone 1 (Z1) and zone 2 (Z2)] in the fruit-bearing branches of 'Elstar' apple trees

Parameter	Treatment					
	Control		LL		LLG	
	Z1	Z2	Z1	Z2	Z1	Z2
Pg_{\max} ($\mu\text{mol CO}_2 \text{ m}^{-2} \text{ s}^{-1}$)						
WAFB 10 (average \pm s.d.)	16.54 \pm 1.15	19.03 \pm 1.45	16.54 \pm 1.15	19.03 \pm 1.45	16.54 \pm 1.15	19.03 \pm 1.45
WAFB 11–24						
Pg_{\max} (WAFB) = $y_0 + ae^{-e^{-(\text{WAFB}-x_0)/b}}$	a	17.8914	17.8914	18.7874	18.9215	10.8351
	b	-3.003	-3.003	-2.7949	-3.4364	-0.9055
	x_0	25.7511	25.7511	25.6347	24.1831	20.3437
	y_0	0	0	0	0	1.6069
Rd ($\mu\text{mol CO}_2 \text{ m}^{-2} \text{ s}^{-1}$) (average \pm s.d.)						
WAFB 10	0.573 \pm 0.094					
WAFB 11–20	0.345 \pm 0.045					
WAFB 21–22	0.440 \pm 0.141					
WAFB 23–24	0.604 \pm 0.210					
α ($\mu\text{mol CO}_2 \mu\text{mol photons}^{-1}$)						
NRH model of Thornley	0.0568 \pm 0.0055	0.0568 \pm 0.0055	–	–	–	–
α (WAFB) = $y_0 + \alpha$ WAFB	a	–	–0.0006	–0.0006	–	–
	y_0	–	0.0629	0.0629	–	–
α (WAFB) = $a/(1 + e^{-(\text{WAFB}-x_0)/b})$	a	–	–	–	0.0563	0.0572
	b	–	–	–	-2.4170	-3.6911
	x_0	–	–	–	24.9279	26.2621
RH model of Thornley						
WAFB 10	0.105 \pm 0.009					
WAFB 11–20	0.0960 \pm 0.0094	0.0960 \pm 0.0094	0.0995 \pm 0.0103	0.0995 \pm 0.0103	0.0927 \pm 0.0081	0.0927 \pm 0.0081
WAFB 21–22	0.0821 \pm 0.0131	0.0821 \pm 0.0131	0.0826 \pm 0.0180	0.0826 \pm 0.0180	0.0656 \pm 0.0148	0.0656 \pm 0.0148
WAFB 23–24	0.0964 \pm 0.0103	0.0964 \pm 0.0103	0.0782 \pm 0.0165	0.0782 \pm 0.0165	0.0723 \pm 0.0163	0.0723 \pm 0.0163
NRH model of Marshall and Biscoe	0.056 \pm 0.011					
θ (dimensionless)						
NRH model of Thornley						
WAFB 10	0.835 \pm 0.049	0.740 \pm 0.097	–	–	–	–
WAFB 11–24	0.721 \pm 0.092					
NRH model of Marshall and Biscoe				0.711 \pm 0.062		
θ (WAFB) = $y_0 + \alpha$ WAFB	a	-0.0130	-0.0098	-0.0199	–	–
	y_0	0.8886	0.7859	0.9880	–	–
θ (WAFB) = $a/(1 + e^{-(\text{WAFB}-x_0)/b})$	a	–	–	–	0.7268	0.7268
	b	–	–	–	-1.7290	-1.7290
	x_0	–	–	–	21.1402	21.1402

TABLE 2. Parameter estimation and preliminary validation of the models used to predict seasonality of net photosynthesis rate

Parameter	Fitting (three trees, $n = 96$)			Preliminary validation (one tree, $n = 32$)		
	R^2_{adj}	d	RMSE	R^2_{adj}	d	RMSEP
Pg_{\max}	0.874	0.967	1.90	0.856	0.963	1.97
Rd	–	0.770	0.12	–	0.540	0.25
α NRH M&B	–	–	0.011	–	–	0.009
α NRH T	0.443	0.779	0.006	0.408	0.738	0.007
α RH T	0.502	0.819	0.011	0.209	0.659	0.014
θ NRH M&B	0.725	0.917	0.095	0.742	0.913	0.095
θ NRH T	–	0.307	0.089	–	0.449	0.090

WAFB (number of weeks after full bloom) was used as the time variable.

The global goodness of the model was evaluated using three statistics: the adjusted coefficient of determination, R^2_{adj} ; root mean squared error, RMSE; and the Willmott index of agreement, d . The predicted capacity was evaluated using the same three indices: R^2_{adj} , d and RMSEP (root mean squared error of prediction).

NRH, non-rectangular hyperbola; RH, rectangular hyperbola; T, Thornley; M&B, Marshall and Biscoe.

leaves (our result showed the end of this phase) were fully photosynthetically active, followed by relatively constant rates until fruit harvest, after which a decline in Pn or Pg_{\max} occurred (Wünsche *et al.*, 2005). At the start of the experiment, Pn_{\max} (or

Pg_{\max}) of vegetative shoot leaves was different between the two zones (Pn_{\max} in Z1 < Pn_{\max} in Z2), then it became non-significantly different (Figs 3 and 4) with time. We cannot rule out the hypothesis that a small developmental delay exists between the

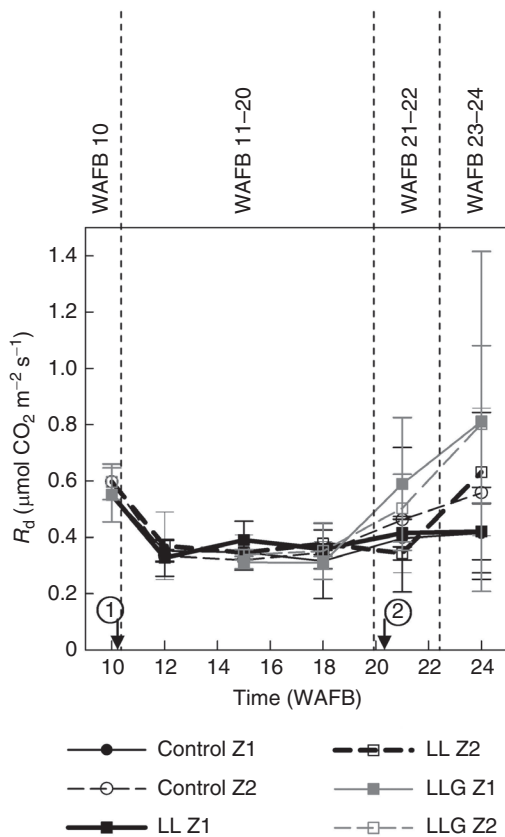


FIG. 5. Time course of R_d (average \pm s.d., $n = 4$) for different fruit load and girdling treatments. The arrow marked 1 indicates application of treatments and that marked 2 indicates fruit harvest. Four periods (WAFB 10, WAFB 11–20, WAFB 21–22 and WAFB 23–24) are indicated.

vegetative shoot leaves in Z1 and the vegetative shoot leaves in Z2. This developmental delay would be the cause of this Pn_{max} decrease in Z1. The selected leaves in Z1 could thus be slightly younger than the leaves in Z2. However, 2 weeks after the beginning of the experiment, that difference had disappeared. Miyazawa *et al.* (2003) put forward the idea that during leaf area expansion in certain plant species there could be competition for nitrogen between cell division and chloroplast development because both processes would be largely nitrogen limited. Both processes would not proceed synchronously due to the limited amount of available nitrogen in the expanding leaves. In *Quercus glauca*, most nitrogen would first be used in the components needed for cell division during leaf area expansion, and thereafter gradually be invested in the photosynthetic apparatus (Miyazawa *et al.*, 2003). Furthermore, anatomical differences in leaves due to the light environment probably contributed in part to the reductions in Pg_{max} of shaded canopy leaves of apple (Campbell *et al.*, 1992). We also observed that the decrease of Pn or Pg_{max} in autumn coincided with the decrease of daily minimum and maximum air temperatures (Figs 2–4). Several studies on a number of species indicated that leaf age, light intensity and temperature could explain this evolution. For rose (*Rosa hybrida*), Gonzalez-Real and Baille (2000) indicate that leaves seem to acclimatize their photosynthetic capacity seasonally, by

TABLE 3. Comparison of the three models (NRH Thornley, RH Thornley and NRH Marshall and Biscoe)

Parameter	Fitting ($n = 864$)			Preliminary validation ($n = 432$)		
	R^2_{adj}	d	RMSE	R^2_{adj}	d	RMSEP
NRH M&B	0.963	0.990	1.182	0.934	0.982	1.575
NRH T	0.960	0.990	1.223	0.930	0.982	1.605
RH T	0.957	0.986	1.362	0.927	0.976	1.735

For more details, see Table 2.

NRH, non-rectangular hyperbola; RH, rectangular hyperbola; T, Thornley; M&B, Marshall and Biscoe.

allocating more photosynthetic nitrogen to leaves in autumn and spring than in summer. von Caemmerer and Farquhar (1984) showed that a change in the light regime for growth from high to low light levels caused a decrease in CO_2 assimilation rate. Furthermore, they infer that changes in the light regime for growth cause parallel changes in ribulose biphosphate (RuBP) carboxylase activity and the ‘capacity for RuBP regeneration’. Finally, the optimum temperature range for photosynthesis in ‘Braestar’ apples is between 25 and 30 °C pre-harvest and between 20 and 25 °C post-harvest (Pretorius and Wand, 2003). At high temperature, the CO_2 assimilation rate was limited by RuBP carboxylation, whereas at low temperature it was limited by RuBP regeneration (Yamori *et al.*, 2010).

Dark respiration progressed with time only (Fig. 5). Overall, the intensity of dark respiration is an indicator of metabolic demand. A high dark respiration during the early growth stages (i.e. WAFB 10) was probably related to the cellular needs that increased and were the site of high synthetic activity. When the organs of the plant grew older and attained maturity (i.e. WAFB 11–20), the growth and the metabolic needs associated with it decreased (Onate and Munné-Bosch, 2009). Next (i.e. WAFB 21–22 and WAFB 23–24), the leaves showed a temporary increase (climacteric peak) of dark respiration. This increase characterized the beginning of leaf senescence and the modifications associated with the degeneration that preceded the death of the leaf (Roux, 1940). No significant effect of zone and treatments on dark respiration was detected in our study, which confirms the study by Fujii and Kennedy (1985) which showed no effect either of fruiting or non-fruiting apple trees on dark respiration of apple. In the work of Fujii and Kennedy (1985), the distribution of fruits within bearing branches was homogeneous. Before harvest, our study is in accordance with their results, while in addition we found that low fruit load and the imbalance of fruit distribution in the same fruit-bearing branch had no significant effect on dark respiration. Our study revealed a higher variability of R_d values after harvest than before harvest (Fig. 5). Furthermore, the advanced discoloration of the leaves in girdled fruit-bearing branches suggests that girdling seems to accelerate the senescence process. Previous work has demonstrated that girdling leads to the accumulation of carbohydrates in leaves and subsequent acceleration of leaf senescence (Krapp and Stitt, 1995; Parrott *et al.*, 2007; Tang *et al.*, 2015, 2016).

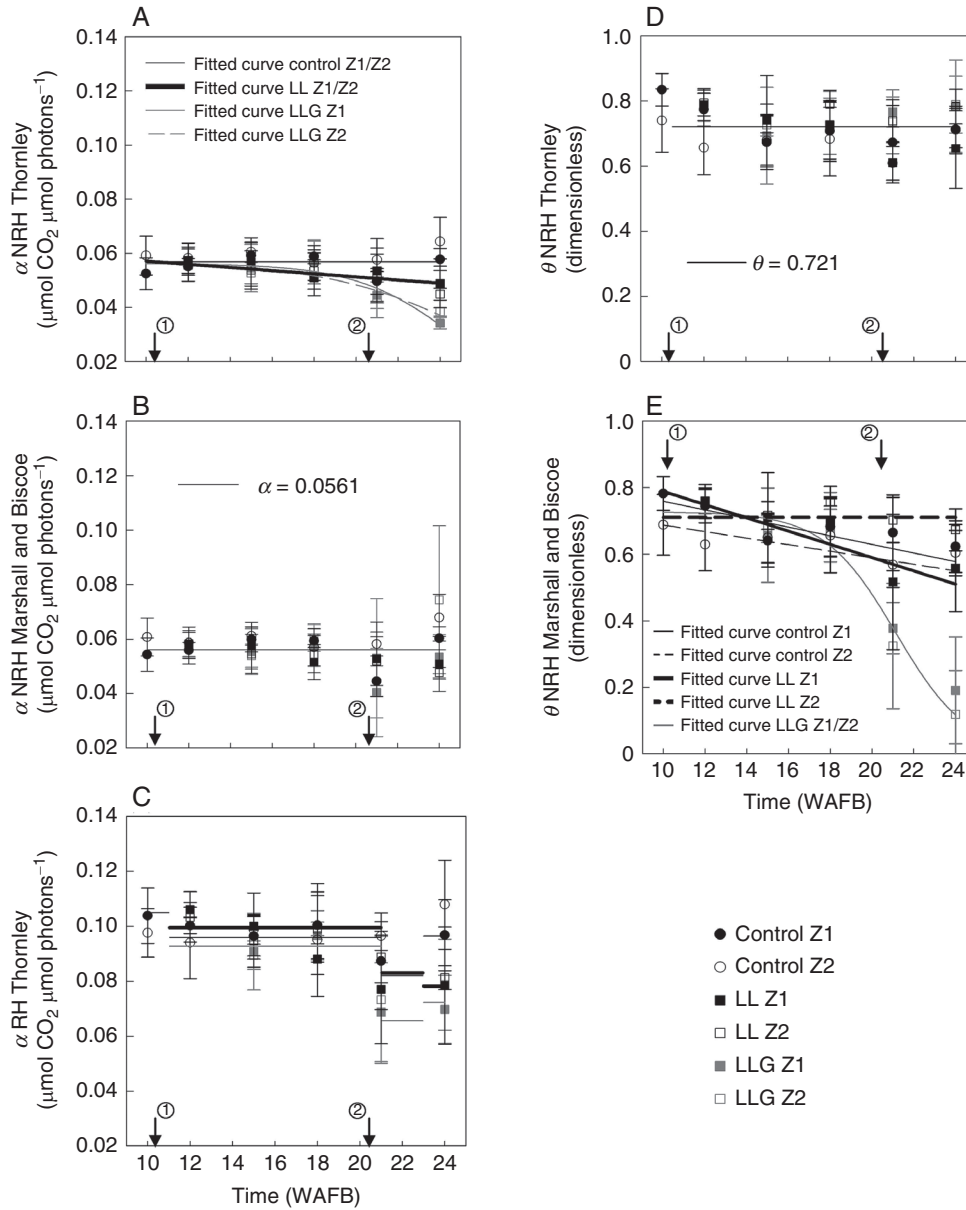


FIG. 6. Modelling of the temporal courses of α (A–C) and θ (D and E)) in Thornley's NRH model (A and D), Marshall and Biscoe's NRH model (B and E) and Thornley's RH model (C) from WAFB 10 to WAFB 24. The arrow marked 1 indicates application of treatments and the arrow marked 2 indicates fruit harvest. Average \pm s.d., $n = 4$ trees. Fitting was done using data from three trees.

Impact of different treatments on sink–source relationships

In this study, 'LL' was a treatment in which fruit load was manipulated in fruit-bearing branches of apple trees in the absence of direct mechanical action on sources and other functional sinks such as roots and stem. We found no significant differences between $P_{n_{\max}}$ in the control and the 'LL' treatments between the onset of the experiment and harvest. This indicated that the sink strength of the developing fruit (or all sinks in the tree), at the scale of the entire tree and/or of the treated bearing branches (Z1 and Z2), was sufficient to generate the same level of $P_{g_{\max}}$ of leaves in the treated bearing branches. This result could indicate that the branch autonomy theory is not suitable to explain sink strength in apple. Furthermore, before harvest,

the heterogeneity in the distribution of sinks (developing fruits) on ungirdled fruit-bearing branches had no effect on the source (leaves of vegetative shoots). In the 'LL' treatment, the absence of sinks after harvest had a negative impact on the $P_{g_{\max}}$ of the leaves in Z1 (zone with fruits) compared with the $P_{g_{\max}}$ of the leaves in Z2 (zone without fruits) (Fig. 4). This result indicates that when the sinks were removed (fruit harvest), the $P_{g_{\max}}$ of the sources that were located in the same zone as the sinks reacted more rapidly than that of the sources that were more distant.

Girdling is a treatment that disturbs or blocks the transport of substances produced in the leaves, to organs and tissues situated upstream of the girdling zone (Sala *et al.*, 2012) and that

influences the rate of photosynthetic assimilation. In another study, it induced an increase of non-structural carbohydrates in the part of the branch situated upstream of the girdling zone (Poirier *et al.*, 2010). The present work (Fig. 3) confirms the negative effect of girdling (feedback inhibition) on the net photosynthesis rate. Furthermore, when the sink organs (fruits) were harvested, the effect of girdling increased drastically. In the present study, the observed reduction of leaf photosynthesis due to leaf reserve accumulation was assumed to be a result of low sink demand (Quilot *et al.*, 2004). A feedback inhibition of leaf light-saturated photosynthesis is correlated with high accumulation of non-structural carbohydrates, such as soluble sugars and starch (Lescourret *et al.*, 1998; Quilot *et al.*, 2004). In a tall conifer, Woodruff and Meinzer (2011) suggest that the accumulation of non-structural carbohydrates (starch, sucrose, glucose and fructose) may be related to constraints on phloem transport.

Model of seasonal variation of Pn: taking into account the effect of treatments

The main purpose of this study was to model the temporal variation (during the growing season) of different parameters ($P_{g_{max}}$, R_d , α and θ) used in the photosynthesis models of Thornley and Marshall and Biscoe, in fruit-bearing branches of apple trees. This study defined the model of Marshall and Biscoe as the most accurate model to simulate the net photosynthesis rate in apple leaves under the experimental and environmental conditions of the present study. The suggested parameters and models allow taking into account the effect of fruit load and girdling in fruit-bearing branches of apple trees by simulating the seasonal and temporal variations of photosynthesis parameters induced by these treatments. The model that we propose in this study is complex, consisting of constant mean values, linear and non-linear models, and is based on temporal (WAFB) and environmental (PAR) variables. As a shortcoming of the present model, one could indicate its narrow range of applicability, i.e. it was fitted and validated (limited validation power, paired data) only on apple trees growing under production conditions based on sufficient water and nitrogen supply and that, at present, it cannot be applied to other experimental conditions as it has not yet been validated. Its advantage is the low number of input variables and the use of climatic and temporal data only.

To conclude, the present study proposed a way to model the photosynthesis rate using temporal and environmental variables only; however, this was done under production conditions, i.e. sufficient water and nitrogen supply in an orchard (sustainable cultural production), using one cultivar and one type of leaf (leaf of a vegetative shoot, Fig. 1D). This model also enabled us to simulate the effect of low fruit load and girdling on the photosynthesis rate, by finding the parameter set for each treatment. A proper validation of the model parameters will be necessary to extend its utilization and appreciate its predictive capacity fully (use of independent data, e.g. data of another year and another environment). One part of this model, i.e. the seasonal and temporal variations of α and θ or the model of Marshall and Biscoe (1980) to simulate the light response curve of the photosynthesis rate, could be used in another photosynthesis model,

e.g. the model of Kim and Lieth (2003), which is more accurate as it allows the prediction of leaf temperature and transpiration.

ACKNOWLEDGEMENTS

This work was supported by ANR contract ANR-14-CE35-0017-01. We sincerely thank the ARCH-E team (IRHS) for making available to us their LICOR portable photosynthesis system. Thanks are also due to the Unité Expérimentale Horticole, Bois-l'Abbé for management of trees.

LITERATURE CITED

- Asao S, Ryan G. 2015. Carbohydrate regulation of photosynthesis and respiration from branch girdling in four species of wet tropical rain forest trees. *Tree Physiology* **35**: 608–620.
- Auzmendi I, Marsal J, Girona J, Lopez G. 2013. Daily photosynthetic radiation use efficiency for apple and pear leaves: seasonal changes and estimation of canopy net carbon exchange rate. *European Journal of Agronomy* **51**: 1–8.
- Binkley D, Stape JL, Takahashi EN, Ryan MG. 2006. Tree girdling to separate root and heterotrophic respiration in two eucalyptus stands in Brazil. *Oecologia* **148**: 447–454.
- von Caemmerer S, Farquhar GD. 1984. Effects of partial defoliation, changes of irradiance during growth, short-term water stress and growth at enhanced $p(\text{CO}_2)$ on the photosynthetic capacity of leaves of *Phaseolus vulgaris* L. *Planta* **160**: 320–329.
- Campbell RJ, Marini RP, Birch JB. 1992. Canopy position affects light response curves for gas exchange characteristics of apple spur leaves. *Journal of the American Society for Horticultural Sciences* **117**: 467–472.
- DeJong TM. 1986. Fruit effects on photosynthesis in *Prunus persica*. *Physiologia Plantarum* **66**: 149–153.
- Dillen SY, Op de Beeck M, Hufkens K, Buonanduci M, Phillips NG. 2012. Seasonal patterns of foliar reflectance in relation to photosynthetic capacity and color index in two co-occurring tree species, *Quercus rubra* and *Betula papyrifera*. *Agricultural and Forest Meteorology* **160**: 60–68.
- Dincer C, Topuz A. 2015. Inactivation of *Escherichia coli* and quality changes in black mulberry juice under pulsed sonication and continuous thermosonication treatments. *Journal of Food Processing and Preservation* **39**: 1744–1753.
- Fan PG, Li LS, Duan W, Li WD, Li SH. 2010. Photosynthesis of young apple trees in response to low sink demand under different air temperature. *Tree Physiology* **30**: 313–325.
- Feng ZZ, Pang J, Kobayashi K, Zhu JG, Ort DR. 2011. Differential responses in two varieties of winter wheat to elevated ozone concentration under fully open-air field conditions. *Global Change Biology* **17**: 580–591.
- Franck N, Vaast P. 2009. Limitation of coffee leaf photosynthesis by stomatal conductance and light availability under different shade levels. *Trees* **23**: 761–769.
- Fujii JA, Kennedy RA. 1985. Seasonal changes in the photosynthetic rate in apple trees: a comparison between fruiting and non-fruiting trees. *Plant Physiology* **78**: 519–524.
- Gonzalez-Real MM, Baille A. 2000. Changes in leaf photosynthetic parameters with leaf position and nitrogen content within a rose plant canopy (*Rosa hybrida*). *Plant, Cell and Environment* **23**: 351–363.
- Grassi G, Vicinelli E, Ponti F, Cantoni L, Magnani F. 2005. Seasonal and interannual variability of photosynthetic capacity in relation to leaf nitrogen in a deciduous forest plantation in northern Italy. *Tree Physiology* **25**: 349–360.
- Hill T, Lewicki P. 2007. *Statistics methods and applications*. Tulsa, OK: StatSoft.
- Högberg P, Nordgren A, Buchmann N, *et al.* 2001. Large-scale forest girdling shows that current photosynthesis drives soil respiration. *Nature* **411**: 789–792.
- Hopkins. 2003. *Physiologie végétale*. Bruxelles: Edn De Boeck Université.
- Iglesias DJ, Lliso I, Tadeo FR, Talon M. 2002. Regulation of photosynthesis through source:sink imbalance in citrus is mediated by carbohydrate content in leaves. *Physiologia Plantarum* **116**: 563–572.

- Janssen PHM, Heuberger PSC. 1995. Calibration of process-oriented models. *Ecological Modelling* **83**: 55–66.
- Kim SH, Lieth JH. 2003. A coupled model of photosynthesis, stomatal conductance and transpiration for a rose leaf (*Rosa hybrid* L.). *Annals of Botany* **91**: 771–781.
- Krapp A, Stitt M. 1995. An evaluation of direct and indirect mechanisms for the ‘sink-regulation’ of photosynthesis in spinach: changes in gas exchange, carbohydrates, metabolites, enzyme activities and steady-state transcript levels after cold-girdling source leaves. *Planta* **195**: 313–323.
- Lescourret F, Ben Mimoun M, Génard M. 1998. A simulation model of growth at the shoot-bearing fruit level I. Description and parameterization for peach. *European Journal of Agronomy* **9**: 173–188.
- Marshall B, Biscoe PV. 1980. A model for C3 leaves describing the dependence of net photosynthesis on irradiance. *Journal of Experimental Botany* **31**: 29–39.
- Mialet-Serra I, Clément-Vidal A, Roupsard O, Jourdan C, Dingkuhn M. 2008. Whole-plant adjustments in coconut (*Cocos nucifera*) in response to sink–source imbalance. *Tree Physiology* **28**: 1199–1209.
- Miyazawa SI, Makino A, Terashima I. 2003. Changes in mesophyll anatomy and sink–source relationships during leaf development in *Quercus glauca*, an evergreen tree showing delayed leaf greening. *Plant, Cell and Environment* **26**: 745–755.
- Nebauer SG, Renau-Morata B, Guardiola JL, Molina RV. 2011. Photosynthesis down-regulation precedes carbohydrate accumulation under sink limitation in *Citrus*. *Tree Physiology* **31**: 169–177.
- Onate M, Munné-Bosch S. 2009. Influence of plant maturity, shoot reproduction and sex on vegetative growth in the dioecious plant *Urtica dioica*. *Annals of Botany* **104**: 945–956.
- Palmer JW. 1992. Effects of varying crop load on photosynthesis, dry matter production and partitioning of ‘Crispin’/M.27 apple trees. *Tree Physiology* **11**: 19–33.
- Palmer JW, Giulliani R, Adams HM. 1997. Effect of crop load on fruiting and leaf photosynthesis of ‘Braeburn’/M.26 apple trees. *Tree Physiology* **17**: 741–746.
- Parrott DL, McInnerney K, Feller U, Fischer AM. 2007. Steam-girdling of barley (*Hordeum vulgare*) leaves leads to carbohydrate accumulation and accelerated leaf senescence, facilitating transcriptomic analysis of senescence-associated genes. *New Phytologist* **176**: 56–69.
- Poirier M. 2008. *Etude écophysiological de l’endurcissement au gel des arbres: impact des conditions estivales de croissance sur la résistance au gel des arbres*. PhD Thesis, Université Blaise Pascal, Clermont-Ferrand, France.
- Poirier M, Lacoite A, Ameglio T. 2010. A semi-physiological model of cold hardening and dehardening in walnut stem. *Tree Physiology* **30**: 1555–1569.
- Pretorius JJB, Wand SJE. 2003. Late-season stomatal sensitivity to microclimate is influenced by sink strength and soil moisture stress in ‘Braestar’ apple trees in South Africa. *Scientia Horticulturae* **98**: 157–171.
- Proietti P. 2000. Effect of fruiting on leaf gas exchange in olive (*Olea europaea* L.). *Photosynthetica* **38**: 397–402.
- Proietti P, Tombesi A. 1990. Effect of girdling on photosynthetic activity in olive leaves. *Acta Horticulturae* **286**: 215–218.
- Quilot B, Génard M, Kervella J. 2004. Leaf light-saturated photosynthesis for wild and cultivated peach genotypes and their hybrids: a simple mathematical modelling analysis. *Journal of Horticultural Science and Biotechnology* **79**: 546–553.
- Roux ER. 1940. Respiration and maturity in peaches and plums. *Annals of Botany* **4**: 317–327.
- Sala A, Woodruff DR, Meinzer FC. 2012. Carbon dynamics in trees: feast or famine? *Tree Physiology* **32**: 764–775.
- Sun J, Sun J, Feng Z. 2015. Modelling photosynthesis in flag leaves of winter wheat (*Triticum aestivum*) considering the variation in photosynthesis parameters during development. *Functional Plant Biology* **42**: 1036–1044.
- Tang G, Li X, Lin L, Guo H, Li L. 2015. Combined effects of girdling and leaf removal on fluorescence characteristic of *Alhagi sparsifolia* leaf senescence. *Plant Biology* **17**: 980–989.
- Tang GL, Li XY, Lin LS, Zeng FJ. 2016. Impact of girdling and leaf removal on *Alhagi sparsifolia* leaf senescence. *Plant Growth Regulation* **78**: 205–216.
- Thornley JHM. 1998. Dynamic model of leaf photosynthesis with acclimation to light and nitrogen. *Annals of Botany* **81**: 421–430.
- Urban L, Léchaudel M, Lu P. 2004. Effect of fruit load and girdling on leaf photosynthesis in *Mangifera indica* L. *Journal of Experimental Botany* **55**: 2075–2085.
- Wang Q, Iio A, Tenhunen J, Kakubari Y. 2008. Annual and seasonal variations in photosynthetic capacity of *Fagus crenata* along an elevation gradient in Naeba Mountains, Japan. *Tree Physiology* **28**: 277–285.
- Weissgerber TL, Milic NM, Winham SJ, Garovic VD. 2015. Beyond bar and line graphs: time for a new data presentation paradigm. *PLoS Biology* **13**: e1002128.
- Willmott CJ. 1982. Some comments on the evaluation of model performance. *Bulletin of the American Meteorological Society* **63**: 1309–1313.
- Wilson KB, Baldocchi DD, Hanson PJ. 2001. Leaf age affects the seasonal pattern of photosynthetic capacity and net ecosystem exchange of carbon in a deciduous forest. *Plant, Cell and Environment* **24**: 571–583.
- Woodruff DR, Meinzer FC. 2011. Water stress, shoot growth and storage of non-structural carbohydrates along a tree height gradient in a tall conifer. *Plant, Cell and Environment* **34**: 1920–1930.
- Wünsche JN, Greer DH, Laing WA, Palmer JW. 2005. Physiological and biochemical leaf and tree responses to crop load in apple. *Tree Physiology* **25**: 1253–1263.
- Xu LK, Baldocchi DD. 2003. Seasonal trends in photosynthetic parameters and stomatal conductance of blue oak (*Quercus douglasii*) under prolonged summer drought and high temperature. *Tree Physiology* **23**: 865–877.
- Yamori W, Evans JR, Von Caemmerer S. 2010. Effects of growth and measurement light intensities on temperature dependence of CO₂ assimilation rate in tobacco leaves. *Plant, Cell and Environment* **33**: 332–343.
- Yang XS, Chen GX, Yuan ZY. 2013. Photosynthetic decline in ginkgo leaves during natural senescence. *Pakistan Journal of Botany* **45**: 1537–1540.
- Zhou R, Quebedeaux B. 2003. Changes in photosynthesis and carbohydrate metabolism in mature apple leaves in response to whole plant source–sink manipulation. *Journal of the American Society of Horticultural Science* **128**: 113–119.